

## Transmutation of Technetium in the Petten High Flux Reactor: A Comparison of Measurements and Calculations

R. J. M. Konings,\* J. L. Kloosterman, J. A. Hendriks, and H. Gruppelaar

*Netherlands Energy Research Foundation ECN, P.O. Box 1, 1755 ZG Petten, The Netherlands*

*Received February 3, 1997*

*Accepted June 30, 1997*

**Abstract**—*Within the frame of the EFTTRA (Experimental Feasibility of Targets for TRAnsmutation) cooperation, rods of  $^{99}\text{Tc}$  metal are irradiated in the Petten High Flux Reactor for 193 effective full power days, during which  $\sim 6\%$  of the  $^{99}\text{Tc}$  is transmuted to the stable  $^{100}\text{Ru}$ . The radial and axial ruthenium distributions in one of the rods are measured by electron probe microanalysis. In the radial direction, the ruthenium concentration strongly increases in the outer rim of the sample, while the axial distribution shows little variation. The average ruthenium concentration, as measured by isotope dilution mass spectrometry, is  $(6.4 \pm 0.2)\%$  at 5 mm from the bottom of the rod and  $(6.1 \pm 0.2)\%$  at 5 mm from the top. The ruthenium concentrations calculated by the KENO three-dimensional Monte Carlo code, 6.1% at 5 mm from the bottom of the rod and 5.7% at 5 mm from the top, are in reasonable agreement with the measured ones. However, the calculated radial distribution of the ruthenium concentration does not agree with the measurements. The radial profile calculated by the MCNP Monte Carlo code, which uses a pointwise cross-section library, agrees much better with the measurements.*

### INTRODUCTION

The long-lived fission product  $^{99}\text{Tc}$  is among the most important nuclides that dominate the beta activity of spent fuel after a hundred thousand years. Because of its high solubility in (ground)water, technetium is easily transported to the biosphere once it is released from the deep-geological waste repository. To reduce the dose risks to future generations, technetium is one of the fission products that should be partitioned from the spent fuel and treated separately, e.g., transmuted in nuclear reactors or conditioned by chemical immobilization.

In 1992, the EFTTRA (Experimental Feasibility of Targets for TRAnsmutation) collaboration was founded between Commissariat à l'Énergie Atomique (CEA), Netherlands Energy Research Foundation ECN, Electricité de France, Forschungszentrum Karlsruhe, Institute for Advanced Materials, and the Institute for Transuranium Elements (ITU), with the aim to investigate experimentally the behavior of targets during irradiation in fast and thermal nuclear reactors and to demonstrate the applicability of scenarios for the transmutation of long-lived fis-

sion products and minor actinides.<sup>1,2</sup> One of the first experiments of EFTTRA has been the irradiation of six metallic technetium rods in the Petten thermal High Flux Reactor (HFR). During this irradiation, the long-lived  $^{99}\text{Tc}$  is transmuted to the stable  $^{100}\text{Ru}$ . This paper describes the comparison of measured and calculated ruthenium concentrations and profiles obtained from postirradiation examinations (PIEs) and three-dimensional Monte Carlo calculations, respectively.

### TARGET CHARACTERIZATION AND IRRADIATION CONDITIONS

The technetium sample was a 4.8-mm-diam, 25-mm-long rod of technetium metal, which was fabricated at the ITU in Karlsruhe, Germany, as part of a series of six. Details of the fabrication method are described in Ref. 3. The density was higher than 99.9% of the theoretical density. Analysis by glow-discharge mass spectrometry showed that the ruthenium concentration in the metal was  $<1$  part per million.

In the EFTTRA-T1 irradiation experiment, three technetium targets were irradiated, each containing two rods,

\*E-mail: konings@ecn.nl

enclosed in a 15.15 titanium stainless steel capsule (Phenix cladding material) provided by CEA. The targets were positioned in peripheral holes of an aluminum sample holder. Three holes were filled with the <sup>99</sup>Tc targets, and the other six holes were filled with iodine targets. The sample holder was placed in an aluminum filler element and loaded in the core position C5 of the Petten HFR. At this position, the total neutron flux in the targets exceeded  $1 \times 10^{15} \text{ cm}^{-2} \cdot \text{s}^{-1}$  with a thermal component higher than  $2 \times 10^{14} \text{ cm}^{-2} \cdot \text{s}^{-1}$ . Fluence detectors (<sup>59</sup>Co and <sup>56</sup>Fe) and gamma scan wires were located close to the technetium targets to monitor the thermal and fast neutron fluences. Also, nine thermocouples were installed to measure the temperature of the facility. The geometry of the irradiation facility is shown in Fig. 1.

The irradiation lasted for eight cycles (192.95 effective full power days in total) and ended at the beginning of 1995. Due to gamma heating, the temperature of the rods exceeded 900 K. At the end of the irradiation, the thermal neutron fluence ( $E < 0.7 \text{ eV}$ ) averaged over the technetium rods reached a value of  $3 \times 10^{21} \text{ cm}^{-2}$ , and the total neutron fluence reached a value of  $2 \times 10^{22} \text{ cm}^{-2}$ .

POSTIRRADIATION EXAMINATIONS

Electron probe microanalysis (EPMA) has been used to measure the radial profiles of the ruthenium concentration at two radial intersections of the rod, section D1

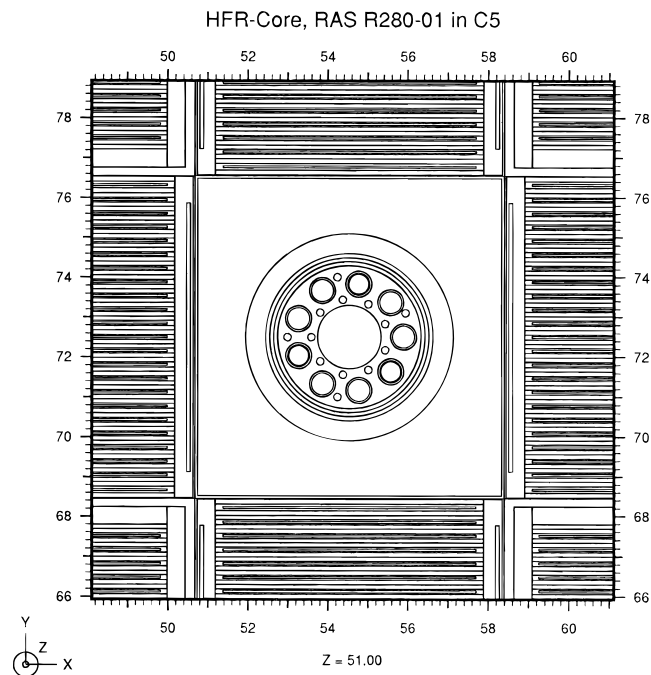


Fig. 1. Horizontal cross section of the irradiation facility surrounded by HFR fuel assemblies.

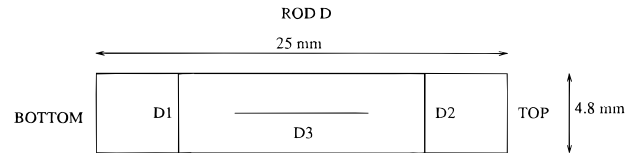


Fig. 2. Drawing of the <sup>99</sup>Tc rod with intersections D1, D2, and D3.

located at 5 mm from the bottom and section D2 at 5 mm from the top, and one axial section, D3, situated between D1 and D2 (see Fig. 2). This was done on a CAMECA MS46R apparatus operating at 20 kV and 40 nA using ruthenium metal as standard.

The ruthenium concentration as a function of the cross-sectional area of the rod at section D1 is shown in Fig. 3. The two curves are the results of two measurements at different azimuthal angles perpendicular to each other. The vertical line at an area of 18.1 mm<sup>2</sup> denotes the outer edge of the rod with a diameter of 4.8 mm. The results at intersection D2, also shown in Fig. 3, are very similar to the ones for section D1. Both figures show the steep increase in the ruthenium concentration in the rim of the pellet, which is caused by the resonance shielding of the neutrons. The difference in the ruthenium concentrations at the outer edge of the rod for measurements 1 and 2 of each profile is most probably due to the position of the sample and the roughness of the surface of the rod. The cross-sectional-averaged ruthenium concentration calculated from the EPMA curves is 7.1 and 6.3% at D1 and 7.4 and 6.8% at D2.

The ruthenium concentration at D3 as a function of the axial distance in the rod is shown in Fig. 4. The average ruthenium concentration is ~5.4%. Although there is a relatively large spread in the results, the slope of the linear least-squares fit indicates a small gradient of the ruthenium concentration as a function of the axial distance. According to this fit, the difference between the ruthenium concentrations at sections D1 and D2 along the rod axis would be 0.24%.

The absolute ruthenium concentration at D1 and D2 has been measured by isotope dilution mass spectrometry (IDMS). To this purpose, discs of ~100 mg were dissolved in HNO<sub>3</sub> (7 mol·dm<sup>3</sup>) to which a standard ruthenium solution was added. The ruthenium was distilled from the solution as ruthenium tetroxide and collected in a NaOH solution, in which it was precipitated as ruthenium dioxide (RuO<sub>2</sub>). The dioxide was dissolved in concentrated hydrochloric acid. The ruthenium concentration in this solution was measured by the triple-filament technique, loading the side filaments with 1/2 to 1 μg ruthenium. The masses 100 and 102 were measured, but also mass 97 to correct for the presence of <sup>100</sup>Mo.

The results of the IDMS measurements are given in Table I. The ruthenium concentration is (6.4 ± 0.2)% at

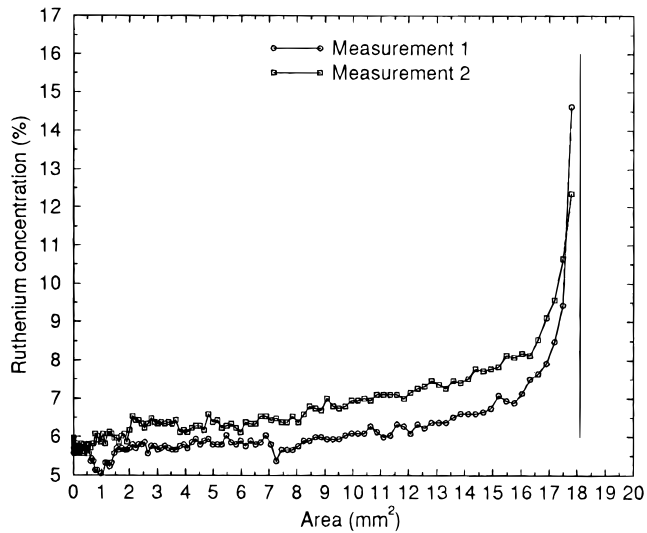
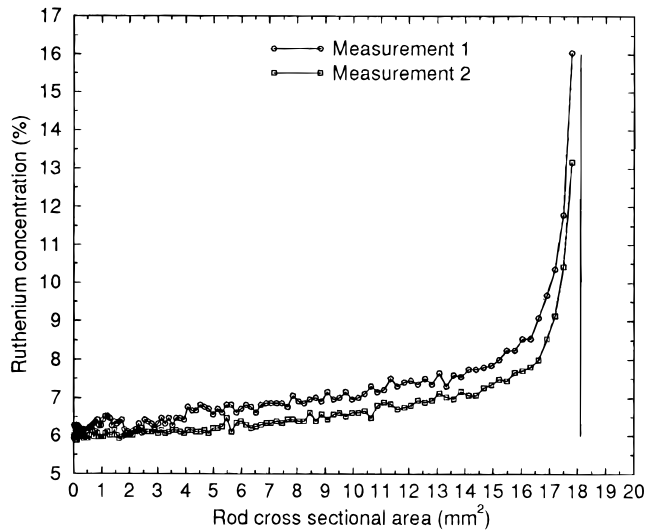


Fig. 3. The profile of the ruthenium concentration at D1 (top) and D2 (bottom) as a function of the cross-sectional area of the rod. The vertical line denotes the outer edge of the rod.

5 mm from the bottom of the rod (D1) and  $(6.1 \pm 0.2)\%$  at 5 mm from the top (D2). Based on these data, the difference between the ruthenium concentrations at sections D1 and D2 is 0.3%.

#### KENO MONTE CARLO CALCULATIONS

To assess the accuracy of the calculational methods and of the nuclear data files used in technetium transmutation studies, calculations have been performed by the KENO-Va Monte Carlo code<sup>4</sup> and associated nuclear data libraries based on the JEF2.2 evaluated file.<sup>5</sup>

The standard three-dimensional core model of the Petten HFR has been used, which implies that the con-

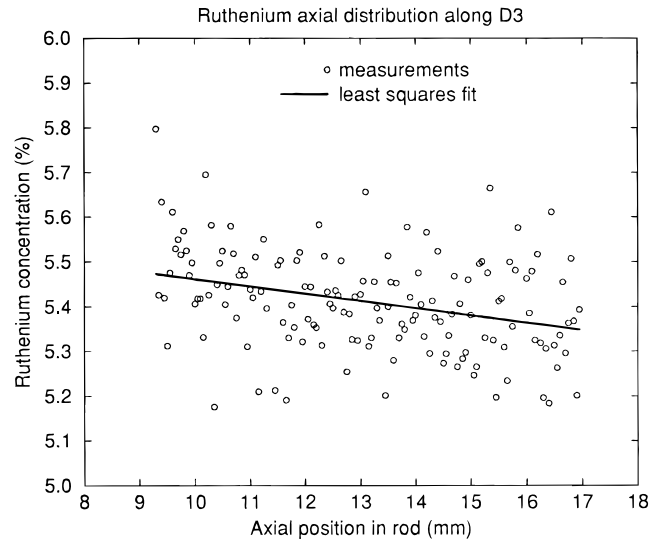


Fig. 4. The profile of the ruthenium concentration at D3 as a function of the axial distance in the rod.

TABLE I

Ruthenium Concentrations at Intersections D1 and D2 Measured by IDMS

Disk	Ruthenium Concentration (%)	
	D1	D2
1	$6.39 \pm 0.15$	$6.13 \pm 0.20$
2	$6.39 \pm 0.24$	$6.18 \pm 0.20$
3		$5.98 \pm 0.24$
Average	$6.39 \pm 0.23$	$6.10 \pm 0.20$

trol members are at a fixed representative position and that a single-type experimental facility was used to fill the experimental positions in the HFR model. This is done because it is too cumbersome to change the core model from one cycle to the other. The influence of these assumptions on the results is probably very small because the experiment itself, which was loaded at position C5, has been modeled accurately, including the details on the fluence detectors (foils) and the gamma scan wires. Also, the three-dimensional fuel distribution has been correctly represented. Figure 5 shows a horizontal cross section of the HFR core model with the experiment loaded at position C5, and Fig. 1 shows the irradiation facility in more detail.

Because a three-dimensional model of the standard HFR core was available for the KENO code, the resonance shielding calculations for all nuclides were performed by the NITAWL-II code<sup>6</sup> (Nordheim method) in the resolved energy region and by the BONAMI-S code<sup>7</sup>

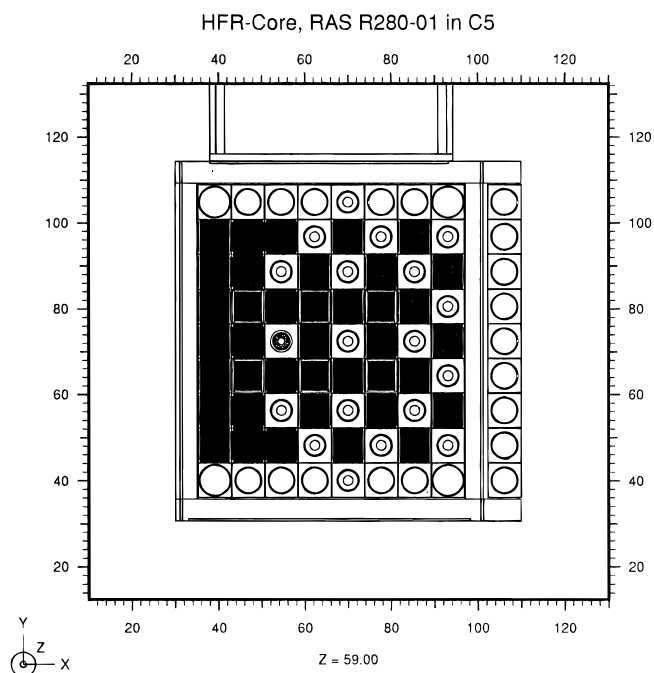


Fig. 5. Horizontal cross-section view of the HFR core model used in the calculations. The experimental facility is loaded at position C5 with  $(x, y)$  coordinates  $(55, 73)$ .

(Bondarenko method) in the unresolved energy region, except for  $^{99}\text{Tc}$ . For this isotope, no resonance shielding in the unresolved region has been performed because of the large background cross sections of  $^{99}\text{Tc}$  in the unresolved region, which may lead to negative cross sections when the resonance shielding is too large. Because the total contribution of the unresolved region to the capture rate is only 6.5%, this has no large effect on the results.

The calculations yield the integrated number of  $^{54}\text{Fe}(n, p)$  and  $^{59}\text{Co}(n, \gamma)$  reactions in the detector foils and the  $^{99}\text{Tc}$  absorption rate as a function of the radius and height of the sample. The ruthenium concentration is then calculated by multiplying the  $^{99}\text{Tc}$  absorption rate with the irradiation time. This is a valid procedure because the technetium concentration does not decrease very much and almost no ruthenium is further transmuted to rhodium ( $^{100}\text{Ru}$  through  $^{102}\text{Ru}$  are stable nuclides and have low absorption cross sections).

The integrated number of  $^{54}\text{Fe}(n, p)$  and  $^{59}\text{Co}(n, \gamma)$  reactions in the detector foils is given in Table II. It is seen that the calculated neutron spectra at the detector positions are quite accurate. The two foils closest to the investigated technetium rod (numbers 6 and 7) give results within 7% for the fast  $^{54}\text{Fe}(n, p)$  reaction and within 1% for the thermal  $^{59}\text{Co}(n, \gamma)$  reaction.

The axial distribution of the ruthenium concentration in the two rods calculated by the KENO Monte Carlo code is shown in Fig. 6 as a function of the axial position in the rods. Also, the two measured values at D1 and D2 are shown. The lower rod ( $0 < z < 25$  mm) has been examined. The vertical bars at each interval denote one standard deviation due to the Monte Carlo process. Clearly, the ruthenium concentration shows an axial gradient, but the volume-averaged ruthenium concentration of the lower rod ( $5.92 \pm 0.01\%$ ) does not differ significantly from that of the upper rod ( $5.87 \pm 0.05\%$ ). These calculations support the measured axial gradient as shown in Fig. 4. The calculated ruthenium concentrations at intersections D1 and D2 are  $(6.10 \pm 0.11)\%$  and  $(5.72 \pm 0.10)\%$ , respectively. These numbers are in reasonable agreement with the measured values given in Table I,  $(6.4 \pm 0.2)\%$  at D1 and  $(6.1 \pm 0.2)\%$  at D2, taking into account the uncertainties in the thermal capture cross section of  $^{99}\text{Tc}$ . According to Ref. 8, the thermal capture cross section of  $^{99}\text{Tc}$  is  $(22.9 \pm 1.3)$  b, which is 10 to 15%

TABLE II

Calculated Reactions in the  $^{54}\text{Fe}$  and  $^{59}\text{Co}$  Detector Foils and the Associated Calculated-to-Experimental Ratios

Detector Foil	$^{54}\text{Fe}(n, p)$ ( $1 \times 10^{21} \text{ cm}^{-2}$ )	C/E* Ratio	$^{59}\text{Co}(n, \gamma)$ ( $1 \times 10^{21} \text{ cm}^{-2}$ )	C/E Ratio
1	$4.84 \pm 0.10$	$1.02 \pm 0.02$	$3.67 \pm 0.05$	$1.03 \pm 0.02$
2	$4.80 \pm 0.10$	$1.01 \pm 0.02$	$3.66 \pm 0.05$	$1.02 \pm 0.01$
3	$4.89 \pm 0.10$	$1.03 \pm 0.02$	$3.63 \pm 0.06$	$0.97 \pm 0.02$
4	$4.94 \pm 0.10$	$1.05 \pm 0.02$	$3.67 \pm 0.05$	$1.01 \pm 0.01$
5	$5.10 \pm 0.10$	$1.08 \pm 0.02$	$3.69 \pm 0.06$	$1.01 \pm 0.02$
6	$5.05 \pm 0.10$	$1.07 \pm 0.02$	$3.57 \pm 0.05$	$1.00 \pm 0.01$
7	$4.86 \pm 0.10$	$1.03 \pm 0.02$	$3.58 \pm 0.05$	$1.01 \pm 0.01$
8	$5.02 \pm 0.10$	$1.05 \pm 0.02$	$3.63 \pm 0.05$	$1.01 \pm 0.01$
9	$5.06 \pm 0.10$	$1.07 \pm 0.02$	$3.57 \pm 0.05$	$0.99 \pm 0.01$
Average		$1.05 \pm 0.02$		$1.01 \pm 0.02$

\*C/E = calculated-to-experimental.

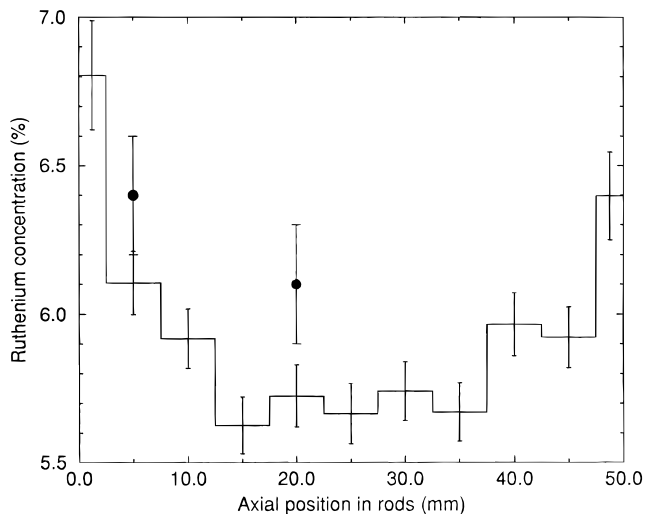


Fig. 6. The calculated ruthenium concentration as a function of the axial position in the rods. The dots indicate the measurement value at D1 and D2.

higher than the value in the JEF2.2 evaluated nuclear data file ( $\sim 19$  b).

The radial distribution of the ruthenium concentration averaged over the two rods in axial direction is shown in Fig. 7. Clearly, the distribution calculated by KENO is not in agreement with the EPMA measurements. Most probably, this is due to the resonance shielding method used in the resolved energy range. By using the Nordheim method, pin-averaged group cross sections are cal-

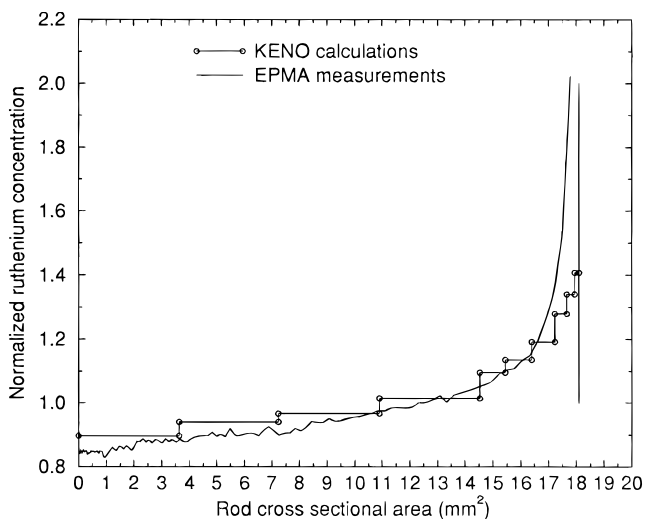


Fig. 7. Comparison of the measured and calculated profile in the rod.

culated, which conserve the total neutron absorption. However, due to resonance absorption, the group cross sections change as a function of the distance to the moderator/rod interface.

To demonstrate the inadequacy of the Nordheim resonance shielding method for these purposes, a model has been defined in which the experiment is represented by five concentric cylindrical zones surrounded by two cuboid zones. The cylindrical zones represent the technetium sample, the homogenized gap, the cladding, the homogenized aluminum sample holder and iodine samples, and the containment. The cuboid zones represent the square element and the other fuel assemblies surrounding the experiment. The zone containing the homogenized samples does not contain the other technetium samples in order not to overestimate the resonance absorption by the technetium in this zone.

The radial distribution of the ruthenium concentration has been calculated by both the KENO and the MCNP-4A (Ref. 9) Monte Carlo codes. The latter code uses a pointwise cross-section library also based on the JEF2.2 nuclear data file. The results are shown in Fig. 8, where the radial distribution of the ruthenium concentrations normalized to the same value is shown together with the results of the EPMA measurements. The KENO results presented in Fig. 8 are almost identical to the three-dimensional results (Fig. 7) that show the adequacy of the cylindrical model. Clearly, the MCNP results are in much better agreement with the measurements than the KENO results, due to the pointwise sampling of the cross sections.

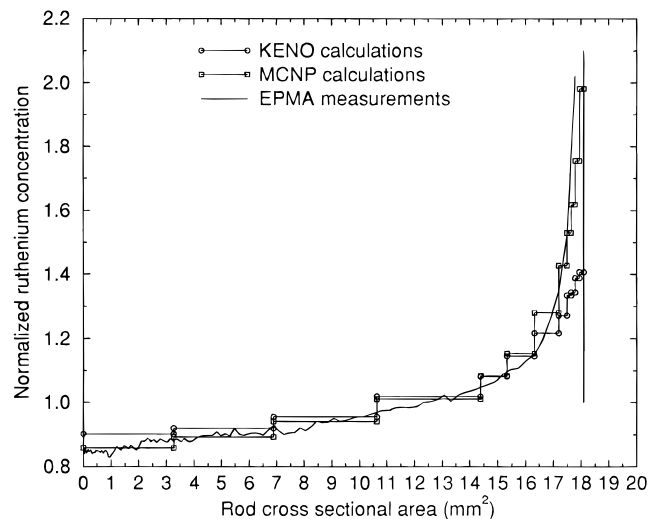


Fig. 8. The radial profile of the ruthenium concentration calculated by KENO, MCNP, and measured by EPMA. The measured curve is the average of the four curves shown in Fig. 3.



## CONCLUSIONS

Samples of metallic  $^{99}\text{Tc}$  have been irradiated in the Petten thermal HFR with a total neutron fluence of  $2 \times 10^{22} \text{ cm}^{-2}$ . During this irradiation, the  $^{99}\text{Tc}$  is transmuted to the stable  $^{100}\text{Ru}$ . The absolute ruthenium concentrations in the rod have been measured by IDMS, and the radial and axial profiles of the ruthenium concentration have been measured by EPMA. The measured ruthenium concentration in the rod ranges from 6.4% at 5 mm from the bottom of the rod (section D1) to 6.1% at 5 mm from the top (section D2).

Calculations have been performed by the groupwise KENO Monte Carlo code in a detailed three-dimensional model of the HFR core. The calculated ruthenium concentrations of 6.1% at section D1 and 5.7% at D2 are in reasonable agreement with the measurements. This shows the validity of the HFR core model and of the cross sections used.

The groupwise KENO Monte Carlo code in combination with the cross-section generation code NITAWL-II (Nordheim resonance shielding method) cannot be used to calculate accurately the radial distribution of the ruthenium concentration in the rods. A Monte Carlo code using pointwise cross sections like MCNP appears to give much better results.

Further work on the transmutation of  $^{99}\text{Tc}$  consists of the reirradiation of two  $^{99}\text{Tc}$  rods in the Petten HFR up to a transmutation level of  $>20\%$  and the measurement of the thermal absorption cross section<sup>10</sup> to verify the number reported in Ref. 8.

## ACKNOWLEDGMENTS

F. van den Berg is acknowledged for performing EPMA and J. G. van Raaphorst for the IDMS analysis.

## REFERENCES

1. J. F. BABELOT, R. CONRAD, W. M. P. FRANKEN, J. VAN GEEL, H. GRUPPELAAR, G. MÜHLING, C. PRUNIER, M. ROME, and M. SALVATOIRES, "Target Develop-

ment and Transmutation Experiments in the Frame of the EFTTRA European Collaboration," *Proc. GLOBAL 1995*, Versailles, France, 1995, p. 524.

2. J. F. BABELOT, R. CONRAD, H. GRUPPELAAR, G. MÜHLING, C. PRUNIER, M. SALVATOIRES, and G. VAMBENEPE, "EFTTRA Irradiation Experiments for the Development of Fuels and Targets for the Transmutation," *Proc. 4th NEA P&T Information Exchange Mtg.*, Mito, Japan.

3. R. J. M. KONINGS, W. M. P. FRANKEN, R. P. CONRAD, J.-F. GUEUGNON, and J.-C. SPIRLET, "Transmutation of Technetium and Iodine—Irradiation Tests in the Frame of the EFTTRA Cooperation," *Nucl. Technol.*, **117**, 293 (1997).

4. L. M. PETRIE and N. F. LANDERS, "KENO-V.a, An Improved Monte Carlo Criticality Program with Supergrouping," Oak Ridge National Laboratory (1989).

5. R. C. L. VAN DER STAD, P. F. A. DE LEEGE, and J. OPPE, "EIJ2-XMAS Contents of the JEF2.2 Based Neutron Cross Section Library in the XMAS Group Structure," ECN-CX-95-087, Netherlands Energy Research Foundation (1996).

6. N. M. GREENE et al., "NITAWL-II, SCALE Module for Performing Resonance Shielding and Working Library Production," Oak Ridge National Laboratory (1989).

7. N. M. GREENE, "BONAMI-S, Resonance Self-Shielding by the Bondarenko Method," Oak Ridge National Laboratory (1989).

8. H. HARADA, S. NAKAMURA, T. KATOH, and Y. OGATA, "Measurement of Thermal Neutron Cross Section and Resonance Integral of the Reaction  $^{99}\text{Tc}(n, \gamma)^{100}\text{Tc}$ ," *J. Nucl. Sci. Technol.*, **32**, 395 (1995).

9. "MCNP-4A: A General Monte Carlo Code for Neutron and Photon Transport," LA-7396-M, Rev. 2, J. F. BRIESMEISTER, Ed., Los Alamos National Laboratory (1986).

10. F. GUNSING, F. STECHER-RASMUSSEN, J. KOPECKY, H. GRUPPELAAR, and H. WEIGMANN, "The Thermal Neutron Capture Cross Section of  $^{99}\text{Tc}$ ," *Proc. Int. Conf. Nuclear Data for Science and Technology*, Trieste, Italy, May 19–24, 1997.